JOURNAL OF GEOPHYSICAL RESEARCH, VOL. 112, C06016, doi:10.1029/2006JC003817, 2007

Asymptotic behavior of frequency and wave number spectra of nearshore shoaling and breaking waves

James M. Kaihatu,[1] Jayaram Veeramony,[2] Kacey L. Edwards,[3] and James T. Kirby[4]

Received 12 July 2006; revised 13 March 2007; accepted 11 April 2007; published 20 June 2007.

[1] Wave number spectra from shoaling and breaking waves in five laboratory tests are compared to a recently published parameterization describing the evolutionary characteristics of surf zone wave spectra. This parameterization proposes two regions in which different wave number spectral shapes are present; the Zakharov range ($2.5\ k_p \leq k \leq 1/h$) has a $k^{-4/3}$ dependence, while the Toba range ($k > 1/h$) has a $k^{-5/2}$ shape. Comparison to laboratory data reveals that the spectral slopes from the Zakharov range of the data trend toward increased agreement with the parameterization in the range of incipient breaking. In contrast, the spectral slopes from the Toba range evolve slowly, likely owing to nonlinear interactions with lower, more energetic wave numbers. However, in the inner surf zone the spectral shape for both parameterized ranges tend toward k^{-2} (or equivalently, f^{-2} in shallow water). The dissipation coefficient $\alpha(f)$ is extracted from time series of free surface elevations; it is found that $\alpha(f)$ has a reciprocal frequency dependence with that of the frequency spectra $S(f)$ of the data, and that this correspondence increases as the waves enter the surf zone. Additionally $\alpha(\mathrm{f}) \sim 1/S(f) \sim f^2$ in the inner surf zone. It is concluded that the wave number spectrum parameterization, particularly in the Zakharov range, reasonably describes the spectral shape while the surf zone is still only partially saturated. However, continued breaking moves the spectral shape away from the parameterized slope toward a f^{-2} (or k^{-2}) spectral shape, representative of the sawtooth-like shape of surf zone waves. This spectral shape is a clear inner surf zone asymptote.

Citation: Kaihatu, J. M., J. Veeramony, K. L. Edwards, and J. T. Kirby (2007), Asymptotic behavior of frequency and wave number spectra of nearshore shoaling and breaking waves, *J. Geophys. Res.*, *112*, C06016, doi:10.1029/2006JC003817.

1. Introduction

[2] The shape and energy content of ocean surface wave spectra in the nearshore zone evidence strong spatial variations on the order of a few wavelengths. Such processes as shoaling, breaking and triadic nonlinear interactions impose strong evolutional variability on the spectrum.

[3] Predictive capability for nearshore waves is accurately provided by Boussinesq-type models, both in frequency domain [*Freilich and Guza*, 1984; *Herbers and Burton*, 1997] and in the time domain [*Madsen et al.*, 1991; *Nwogu*, 1993; *Wei et al.*, 1995; *Kennedy et al.*, 2000]. For accurate spectral modeling of the high-frequency range of the spectrum, recourse can be made to fully dispersive nonlinear models [*Agnon et al.*, 1993; *Kaihatu and Kirby*, 1995; *Agnon and Sheremet*, 1997; *Kaihatu*, 2001] or to extended Boussinesq models in the frequency domain [*Chen and Liu*, 1995; *Eldeberky and Battjes*, 1996; *Kaihatu and Kirby*, 1998; *Kofoed-Hansen and Rasmussen*, 1998]. Several of these models have incorporated dissipation by wave breaking, using lumped parameter dissipation models [e.g., *Battjes and Janssen*, 1978; *Thornton and Guza*, 1983] coupled to a frequency distribution function. These models are potentially computationally expensive (though usually not prohibitive) to use since the nonlinear interactions must be explicitly calculated. However, they are able to provide a host of statistical quantities (e.g., skewness, asymmetry) which are potentially useful for sediment transport and morphology calculations [e.g., *Hoefel and Elgar*, 2003; *Lescinski et al.*, 2003].

[4] An alternative approach to representing these processes in a model-based form is to parameterize the physics by reducing the description of the processes to several data-fitted parameters. This is routinely done for simple breaking models [*Battjes and Janssen*, 1978; *Thornton and Guza*, 1983] and has also been used for nonlinear wave-wave interactions in the nearshore [*Eldeberky and Battjes*,

[1]Zachry Department of Civil Engineering, Texas A&M University, College Station, Texas, USA.
[2]Advanced Systems Group, Jacobs Technology Inc., Stennis Space Center, Mississippi, USA.
[3]Oceanography Division, Naval Research Laboratory, Stennis Space Center, Mississippi, USA.
[4]Center for Applied Coastal Research, University of Delaware, Newark, Delaware, USA.

0148-0227/07/2006JC003817$09.00

1995]. Recently, *Smith and Vincent* [2003] (hereafter SV03) developed an equilibrium description of the wave number spectrum of nearshore waves. Building on the work of *Zakharov* [1999] and *Toba* [1973], they developed equilibrium spectra descriptions for the range k > 2.5 k_p, where k is the wave number and k_p is the wave number at the spectral peak. While the concept of equilibrium spectral shapes has been a fixture of deep water wave research [*Phillips*, 1958; *Kitaigorodskii*, 1983; *Resio et al.*, 2001], only *Thornton* [1977] and *Zakharov* [1999] have proposed equilibrium spectra in the nearshore and surf zones prior to SV03. One probable reason for this dearth of work in this area has been the amplification of the second (and higher) harmonic of the spectral peak due to triad interactions; the resulting spatial variability of the spectral shape would make a general parameterization untenable. The nonlinear energy transfer, however, tends to equilibrate any gaps between local peaks in the spectrum [*Elgar et al.*, 1990a]; the high-frequency portion of the spectrum thus evolves into a flat, featureless shape as the waves move through the surf zone [*Herbers and Burton*, 1997]. In this region of the spectrum, parameterization of the evolution of the high-frequency tail is an attractive possibility.

[5] The SV03 parameterization is intended to be descriptive of the relaxation tendencies of transforming and breaking wave spectra. However, it is not clear that behavior of waves in the surfzone is indicative of any sort of relaxation toward thermal equilibrium, which is the foundation of *Zakharov*'s [1999] approach. Waves approaching such a condition should have small asymmetry values, indicating an absence of rapid energy transfer across the frequency spectrum. (Skewness and asymmetry are statistical third moments characterizing wave shape. Skewness is calculated by

$$\text{Skewness} = \frac{\langle \eta^3 \rangle}{\langle \eta^2 \rangle^{\frac{3}{2}}}, \tag{1}$$

where the brackets denote an ensemble average, and is a statistical measure of asymmetry about a horizontal plane. Asymmetry is determined as

$$\text{Asymmetry} = \frac{\langle \mathcal{H}(\eta)^3 \rangle}{\langle \eta^2 \rangle^{\frac{3}{2}}}, \tag{2}$$

where $\mathcal{H}$ denotes the Hilbert transform of the signal, and is a measure of (in this context) asymmetry about a vertical plane.) In contrast, surfzone waves are characterized by large, negative values of asymmetry, indicating a rapid transfer of energy across the spectrum from low to high frequencies. *Zakharov* [1999] suggests that the limits of validity of the theory place a strong constraint on the allowable range of wave heights. Defining a representative amplitude to depth ratio as

$$\delta = \frac{a}{h} \tag{3}$$

and a dispersion parameter

$$\mu = kh. \tag{4}$$

Zakharov's constraint (his equation (7.13)) can be written as

$$\delta \ll \mu^{3/2} \tag{5}$$

or, in terms of an Ursell number,

$$U_r = \frac{\delta}{\mu^2} \ll \mu^{-1/2}. \tag{6}$$

Zakharov discusses values of $\mu = O(0.1)$ as being an appropriate scale for the shallow water formulation. In this range of values, we would need $U_r \ll 3$ or so. However, for surfzone waves δ can easily approach values close to 0.5, and hence Ursell numbers as defined here take on values of $O(50)$, ten times too large for applicability of the theory. If we relax the constraint on smallness of μ, the Ursell number falls to the range of $O(\mu^{-1/2})$ for μ values around 0.5, which is probably too large a range to be representative of surfzone conditions, falling well outside the surfzone for the cases examined below. It is thus doubtful that the asymptotic form suggested by Zakharov is appropriate for describing surfzone waves in a reasonable parameter range.

[6] We thus wish to examine parameterization of wave spectra in a broadened context that includes consideration of the breaking process and the general evolution of wave form as characterized by its third moments. Representation of the dissipation in a generic spectral wave transformation model can be expressed as

$$A_{nx} = -\alpha_n A_n, \tag{7}$$

where A_n is the complex wave amplitude for the nth frequency (f) component and α_n is a dissipation coefficient whose frequency dependence must be assumed. Several studies have investigated the distribution of α_n over the frequency range. *Mase and Kirby* [1992] (hereafter MK92) first used an f^2 dependence of α_n over the frequency range, while *Eldeberky and Battjes* [1996] distributed α_n over the frequency range independent of frequency. *Kirby and Kaihatu* [1996] provide physical reasoning for the f^2 distribution based on the power spectrum of a sawtooth-like waveform, reminiscent of surf zone waves. *Chen et al.* [1997], using a frequency domain Boussinesq model [*Chen and Liu*, 1995] in concert with laboratory and field data, determined that the predicted shape of the power spectrum of the waves was relatively unaffected by the choice of frequency dependence in α_n, indicating that the nonlinearity and dissipation work in concert to maintain some iconic spectral shape. SV03 note that the nonlinear energy transfer would therefore tend to adjust to compensate for an incorrect dissipation function. The consequence for this adjustment in nonlinearity is a deterioration of the accuracy of prediction of wave shape-related statistics such as skewness and asymmetry [*Chen et al.*, 1997], who also determined that an f^2 distribution for α_n led to optimum predictions of skewness and asymmetry.

[7] In this study, we examine the SV03 equilibrium spectra parameterization and show comparisons to five experimental data sets. Using the data we also examine

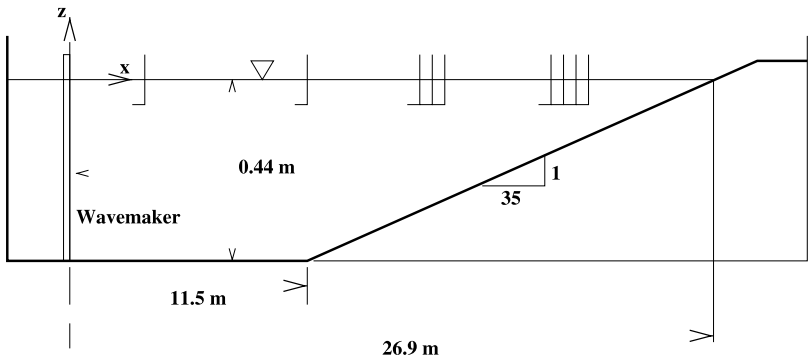

Figure 1. Layout of experiment of *Bowen and Kirby* [1994].

the parameterization relative to other hypotheses on the nature of spectral wave dissipation.

2. Parameterization of *Smith and Vincent* [2003]

[8] *Smith and Vincent* [1992] conducted a laboratory experiment in which random waves were transformed over a sloping bottom in a wave flume. The incident wave conditions included single and multipeaked spectra. They noticed that the higher-frequency peak of the wave spectra would usually disappear as shoaling and breaking continued. Harmonics of the lower frequency peak would temporarily become evident as nonlinear interactions become stronger, but would soon diminish as dissipation becomes more dominant. Eventually, the spectral tail would evidence no harmonic amplification of the spectral peak; the tail would evidence two characteristic slopes when mapped into wave number space. SV03 also noted similar trends in wave spectra measurements taken at the U.S. Army Corps of Engineers Field Research Facility at Duck, NC. On the basis of work by *Zakharov* [1999] and *Toba* [1973], SV03 developed the following parameterizations for $H_{rms}/h > 0.4$:

$$S(k) = \beta_Z k^{-4/3}; kh < 1 \tag{8}$$

$$S(k) = \beta_T k^{-5/2}; kh > 1, \tag{9}$$

where β_Z and β_T are coefficients which can further be made functions of depth h,

$$\beta_Z = \Delta_Z h^{5/3} \tag{10}$$

$$\beta_T = \Delta_T h^{1/2}. \tag{11}$$

These coefficients Δ_Z and Δ_T (and in turn β_Z and β_T) determine the energy level of the wave number spectrum. One of the requirements for the validity of the parameterizations is that $\Delta_Z = \Delta_T$ so that spectral values match at $kh = 1$. Using regression analysis on their data, SV03 found $\Delta_Z = 0.0102$ and $\Delta_T = 0.0103$. We remark here that there is little guidance by which to specify the slope of the high wave number range of the spectrum in or near a surf zone. Evolution of this range of the spectrum is not expected to be dependent on water depth. The parameterization proposed by *Toba* [1973] is for wind-driven deep water waves, not for steep near-breaking and breaking waves in the surf zone. It was, however, adopted by SV03 as part of their equilibrium spectral parameterization. In the spirit of testing this parameterization, we retain the *Toba* [1973] form.

3. Comparison to Experiments

[9] Two laboratory data sets are used to determine possible trends in the evolution of the frequency and wave number spectra of shoaling and breaking waves. We first compare the SV03 parameterization to the wave number spectra from the data. We then determine the best fit slopes of the wave number spectra within both *Zakharov*'s [1999] and *Toba*'s [1973] ranges for each record, and compare them to the values predicted by SV03. We also fit slopes to the corresponding frequency spectra from the experiments to determine their evolution, and then relate them to the dissipation characteristics deduced from the data.

3.1. Description of Data Sets

[10] The first data set described is that of *Bowen and Kirby* [1994] (hereafter BK94), in which single-peaked spectra of random waves were generated and allowed to propagate over a sloping bottom; the experimental layout appears in Figure 1. Three wave conditions were used; these appear in Table 1. A TMA spectrum [*Bouws et al.*, 1985] (see Appendix A) with a width parameter $\gamma = 3.3$ was used for the initial condition at the wave paddle. Data were taken at 47 different locations in the tank, with 44 of them being along the 1 : 35 sloping beach. Ten surface-piercing capacitor wave gages were used at any one time; their locations were changed as each experiment was repeated until the entire domain was covered. The gages sampled at 25 Hz for about 17 min; the first 925 points were discarded to allow the domain to fill up with waves. The remaining 24,076 elevations in each time series were then divided into 12 realizations of 2048 points each. A time-domain Fast

Table 1. Wave Parameters of Experiments

Experiment Name	H_{rms}, m	f_p, Hz
BK94 A	0.07	0.5
BK94 B	0.08	0.225
BK94 C	0.09	0.225
MK92 1	0.04	0.6
MK92 2	0.04	1.0

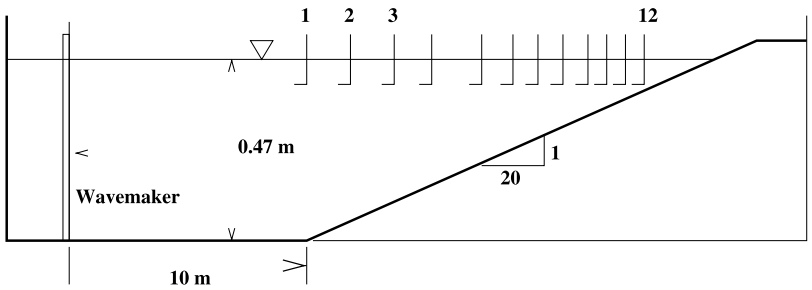

Figure 2. Layout of experiment of *Mase and Kirby* [1992].

Fourier Transform (FFT) was used to calculate the frequency spectrum for each realization. The Nyquist frequency f_{Nyq} = 12.5 Hz. Averaging over the realizations, and then band averaging eight adjacent bands, resulted in frequency spectra with 192 degrees of freedom. We will concentrate on the gages on the slope for our analysis.

[11] The second data set is that of *Mase and Kirby* [1992] (hereafter MK92), which has been used in several studies detailing nonlinear model development [*Mase and Kirby*, 1992; *Kaihatu and Kirby*, 1995; *Eldeberky and Madsen*, 1999; *Kennedy et al.*, 2000; *Kaihatu*, 2001]. In particular, Run 2 of MK92 has served as a testbed for dispersive nonlinear models due to its high relative depth at the wavemaker ($k_p h = 2$, where k_p is the wave number of the spectral peak). Owing to this high relative depth, the Run 2 data would appear to be on the outer edge of suitability for testing the SV03 parameterization. However, spectral evolution and wave breaking in the surf zone do occur, so comparison with SV03 makes for a valid test. The experimental layout showing the locations of the surface-piercing gages appears in Figure 2. A Pierson-Moskowitz (see Appendix A) spectrum was input at the wavemaker; the parameters of the incident wave condition appear in Table 1. Data from Run 1 were sampled at 25 Hz (f_{Nyq} = 12.5 Hz) at eleven gages, then divided into ten realizations of 2048 points apiece. Data from Run 2 were sampled at 20 Hz (f_{Nyq} = 10 Hz) at twelve gages, then divided into seven realizations of 2048 points apiece. After application of the FFT, calculation of the frequency spectra and averaging over realizations, the spectra were further band-averaged over eight adjacent bands, resulting in 160 degrees of freedom for Run 1 and 112 degrees of freedom for Run 2.

[12] We calculated root-mean-square wave height H_{rms}, skewness and asymmetry from the data; these are shown in Figure 3. Skewness generally increases as waves move toward the shoreline, thus reflecting the peaked crests and flatter troughs of nonlinear waves. In contrast, asymmetry generally becomes more negative, indicative of the steep front face and shallow rear face of breaking waves. For both BK94 and MK92, the skewness reaches a maximum, then begins a reduction as the waves approach the shoreline. In contrast, the asymmetry becomes more negative, with a slight reduction in the very nearshore in the BK94 data. The peaking of skewness prior to the shoreline has been demonstrated before for field wave conditions [*Elgar et al.*, 1990b].

[13] The dispersion parameter $\mu_p^2 (= k_p^2 h^2)$ and the nonlinearity parameter $\delta (= H_{rms}/2h)$ were calculated for all experimental data; the result is also shown in Figure 3. The total data set covers the relative depth range out to $\mu_p^2 = 3.4$ and a considerable range of nonlinearity.

3.2. Wave Number Spectra and Determination of Slopes

[14] We calculate the wave number spectra for all time series from all experiments by transformation of the smoothed frequency spectra as follows:

$$S(k) = \frac{C_g(k,f,h)}{2\pi} S(f), \tag{12}$$

where C_g is the group velocity calculated using the wave number from the linear dispersion relation,

$$(2\pi f)^2 = gk \tanh kh. \tag{13}$$

The water depth h used in the calculations does not include wave-induced setup. We also did not account for any bound waves in the higher frequencies; SV03 noted that the Zakharov range data fits were not biased by the use of linear theory for this transformation to wave number spectra.

[15] The slope of each spectrum was calculated by using a linear regression to the log of $S(k)$ and k. For their laboratory data, SV03 chose their Zakharov range between $2.5\ k_p \leq k \leq 1/h$, and their Toba range $k > 1/h$ with no apparent upper limitation, though they only applied the parameterization where $H_{rms}/h \leq 0.4$. SV03 required an upper frequency cutoff for the field data due to the limitations of transforming pressure records to free surface elevations. For the assembled surface elevation data herein, the Zakharov range was defined as $k_p \leq k < 1/h$ and a Toba range $1/h \leq k \leq k(0.5 f_{Nyq})$. These ranges were determined by visually inspecting the smoothed wave number spectra and performing some sensitivity analyses of the resulting wave number spectral slopes on the range limits; the resulting range limits show the parameterization in the best agreement with the data. We note that these ranges are outside those defined by SV03. We also note that the upper limit of the wave number range under consideration is in the capillary-wave range. However, there is not a significant break to a different slope until beyond the present high wave number cutoff. The range of capillary wave motions included in the slope calculations does not have a significant effect on the resulting slope.

3.3. Comparison to SV03

[16] Representative comparisons of the SV03 parameterization with the wave number spectra from several gages of

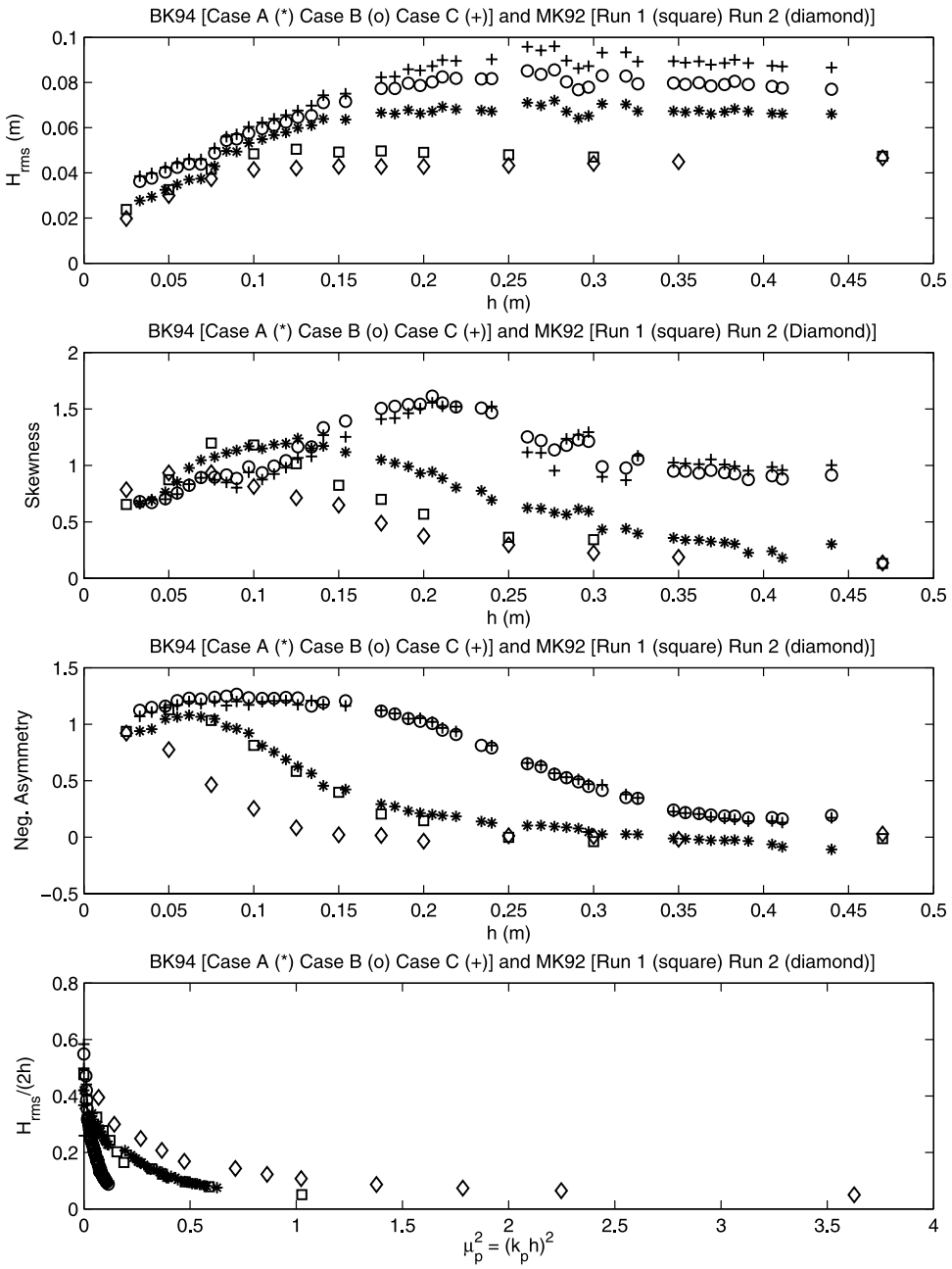

Figure 3. Wave height, third-moment statistics, nonlinearity, and dispersion parameters, data of *Bowen and Kirby* [1994] and *Mase and Kirby* [1992]. Data of *Bowen and Kirby* [1994]: asterisks, Case A; circles, Case B; pluses, Case C. Data of *Mase and Kirby* [1992]: squares, Run 1; diamonds, Run 2.

the experiments are shown in Figures 4 (BK94 Case B) and 5 (for MK92 data Run 2). Best fit slopes of the wave number spectra for the Zakharov and Toba ranges are also determined; these lines also appear in Figures 4 and 5.

[17] For the BK94 Case B experiment (Figure 4), the parameterization's β_Z and β_T coefficients overpredict the spectral energy consistently until the surf zone. This is in line with SV03, who test their parameterization primarily where $H_{rms}/h > 0.4$, a rough indication of the outer edge of the surf zone. Interestingly, the slopes of the Zakharov and Toba ranges of the parameterization appear to match the data quite well outside breaking but agree less in the inner surf ($h < 0.10$ m). This is also seen in the MK92 Run 2 comparisons (Figure 5), though the relaxation of the spectrum to the parameterized values is not as apparent as in BK94. The evolutionary characteristics of the MK92 Run 2 test are very different than those demonstrated by the BK94 Case B data. While the BK94 Case B data reaches an equilibrium state and evidences a long flat extent in the high wave number range, the MK92 Run 2 case clearly continues to evolve even at the last gage. Interestingly, the parameterization does predict the slope break quite well in the two shallowest gages ($h = 0.05$ m and $h = 0.02$ m) of the MK92 Run 2 data.

[18] SV03 did allow that the coefficients of the parameterization would likely require calibration in the case where

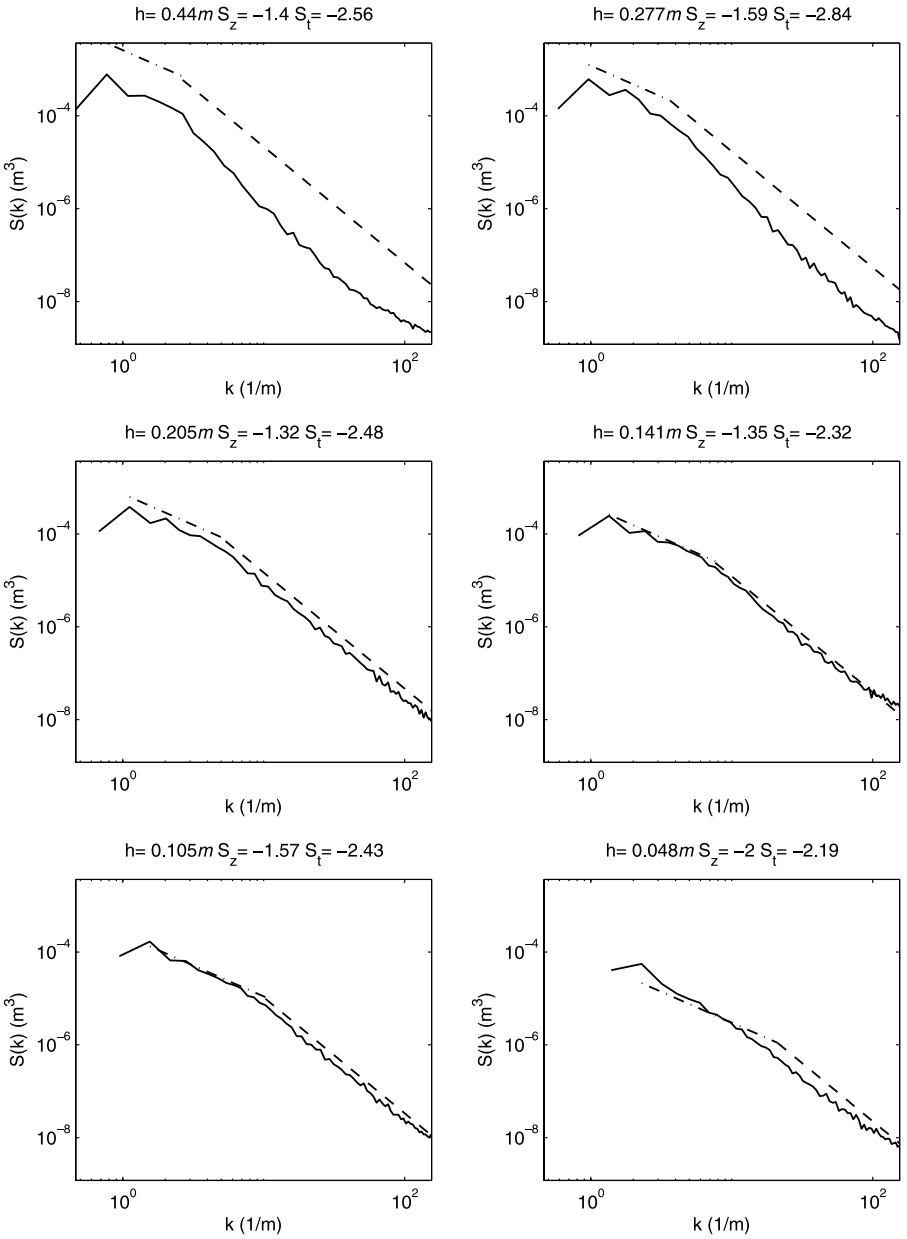

Figure 4. Comparisons of wave number spectra to SV03 parameterization; best fit lines for spectra also shown. Data are BK94 Case B. Solid line is data. Dash-dotted line is SV03, Zakharov range. Dashed line is SV03, Toba range. Slope of best fit line for Zakharov range (S_z) and Toba range (S_t) are shown above each figure, along with water depth h.

there are other effects causing dissipation. For the remainder of this study we will be concerned with the slopes of the parameterization, and their agreement with data, rather than the coefficients.

[19] Figure 6 shows the evolution of the wave number spectral slopes for the Zakharov and Toba ranges as a function of depth for the BK94 and MK92 data; also shown are the values dictated by SV03. For Case A of BK94, the slope of the Zakharov range increases over the domain and approaches the SV03 value, but then decreases away from this value. This trend is more evident for Cases B and C, which have a smaller relative depth at the initializing gage than Case A; the Zakharov range slope follows the SV03 value fairly closely, reaching a maximum near h = 0.2 m before evolving toward a more negative value. The best fit wave number spectra slope of the Toba range, in contrast, does not follow the value prescribed by SV03, but rather appears to reach the SV03 value just as the maximum value of the Zakharov range slope is reached. The gradual nature of this evolution is likely due to slow interactions with more energetic lower wave numbers, and not directly due to the water depth.

[20] It is also apparent from BK94 that the wave number spectral slopes (both Zakharov and Toba ranges) converge near k^{-2}, particularly for Cases B and C. In shallow water, k^{-2} corresponds to f^{-2}. This convergence will be examined

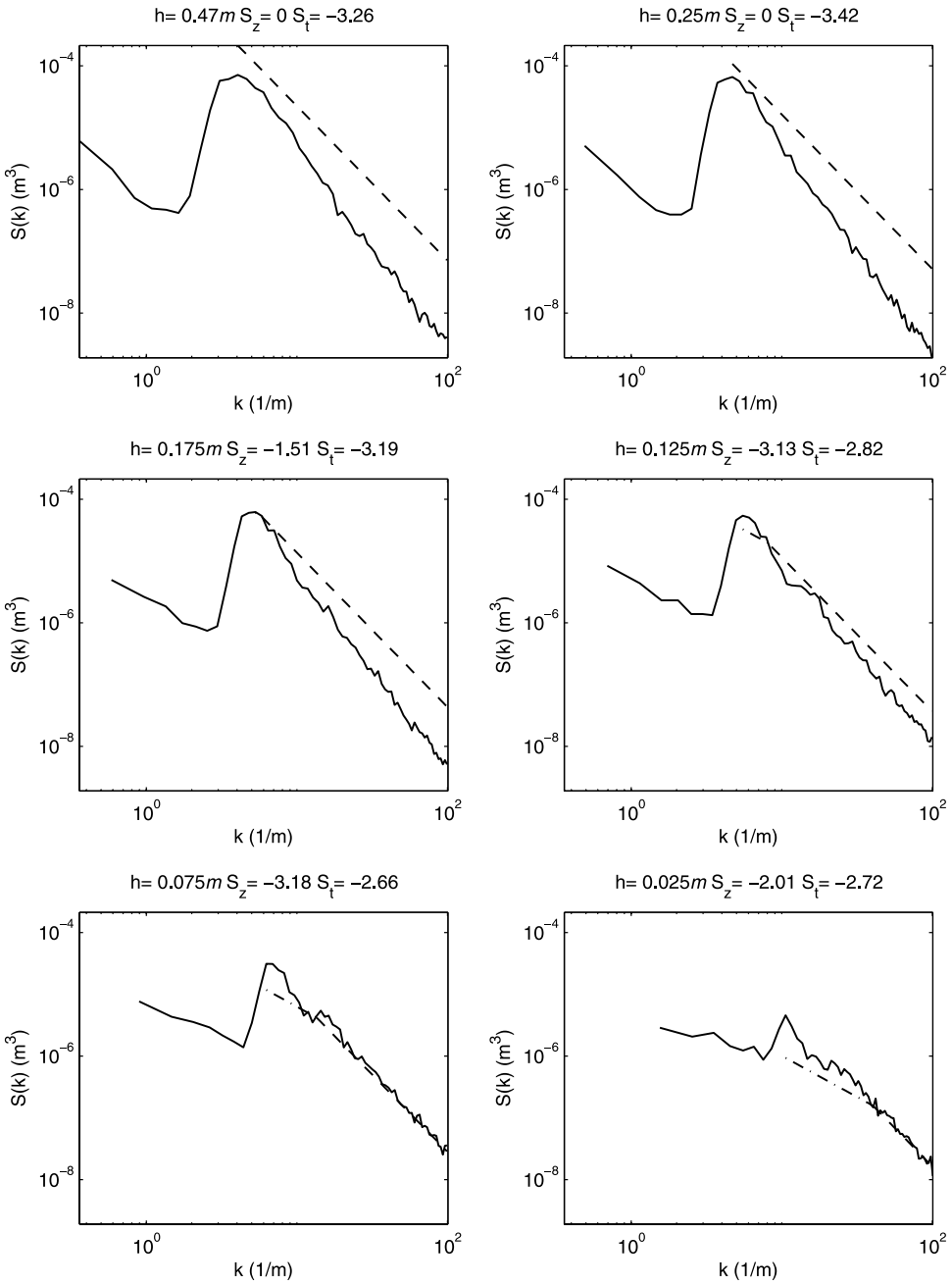

Figure 5. Comparisons of wave number spectra to SV03 parameterization; best fit lines for spectra also shown. Data are MK92 Run 2. Solid line is data. Dash-dotted line is SV03, Zakharov range. Dashed line is SV03, Toba range. Slope of best fit line for Zakharov range (S_z) and Toba range (S_t) are shown above each figure, along with water depth h.

further in a later section. *Kirby and Kaihatu* [1996] argue that an f^{-2} spectral shape implies an f^{-2} dependence for the dissipation coefficient α_n, as discussed in the next section.

[21] These trends are less evident in the MK92 data, likely due to the greater relative depth of the wave condition. One result of the larger relative depth is a nonexistent Zakharov range for most of the domain, since it is only defined if $k_p < 1/h$. However, the MK92 data set still evidences the dynamic nature of the wave number spectral slopes of the Zakharov and Toba ranges. MK92 Run 1 shows the establishment of the Zakharov range around $h = 0.3$ m, and a gradual rise toward the SV03 value near the end of the domain, with a convergence toward k^{-2}. Additionally, the Toba range reaches the SV03 value around $h = 0.125$ m, overshoots it, then falls toward the parameterized value. The Toba range slope for Run 1 comes close to the k^{-2} value, while the Zakharov range slope appears to decrease toward it, except for the final gage. The Toba range slope of Run 2 reaches the parameterized value prior to the last gage. The slope of the Zakharov range for Run 2 does reach k^{-2}, but is built on very few points in the spectrum

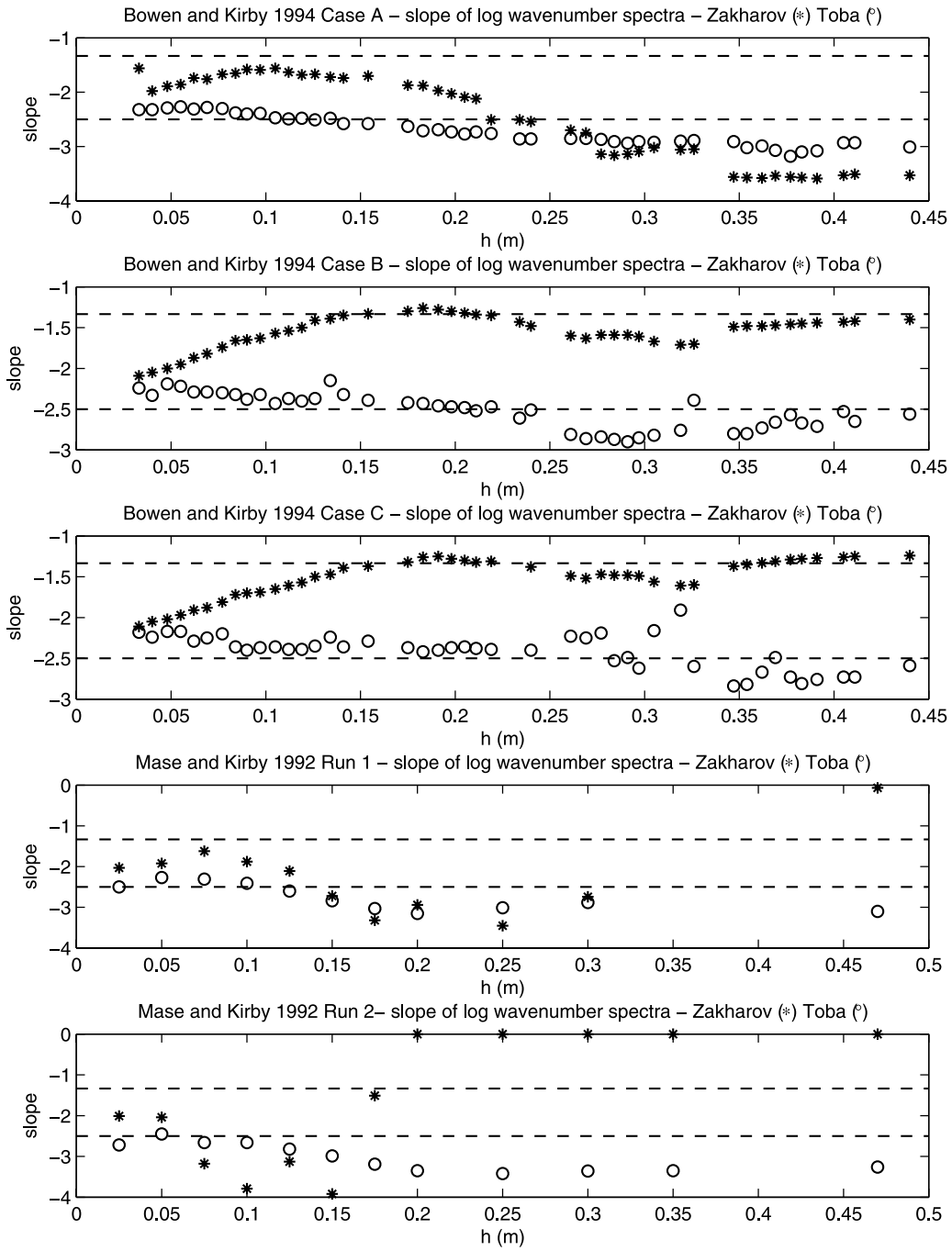

Figure 6. Best fit slopes of the log of the wave number spectra from data as a function of water depth. Asterisks, Zakharov range; circles, Toba range. Slopes from SV03 parameterization are shown in dashed lines.

owing to the high relative water depth, so its accuracy may be called into question.

[22] While the trend toward k^{-2} is clear in the data in the nearshore ends of the experiment, it is somewhat difficult to interpret the trends at the seaward edge of the domain. This is particularly true of the MK92 Run 2 data. Most of the high wave number end of the spectrum is in deep water for a wide range of the domain. The Toba range makes up the majority of the spectral description. In this range, the four-wave interactions, which are much slower than triad interactions, dominate.

4. Frequency Spectra of Breaking Waves

[23] It was mentioned that MK92 and *Kirby and Kaihatu* [1996] hypothesized an f^2 distribution for the dissipation coefficient α_n. The concept of a frequency-dependent dissipation coefficient was tested by incorporation of trial frequency distributions into frequency domain models with

lumped parameter dissipation functions. In these models, the frequency distribution modifies the dissipation function. *Kaihatu and Kirby* [1995], *Chen et al.* [1997], and *Kaihatu* [2001] have all shown that the use of an f^2 dependence gives an accurate reproduction of third-moment wave shape statistics taken from laboratory data.

[24] An alternative to iterative testing of trial distributions would involve evaluation of the power spectrum of the instantaneous dissipation present in a breaking wave field. To achieve this, *Kirby and Kaihatu* [1996] used an eddy-viscosity breaking model [*Zelt*, 1991] to determine the dissipation from data; we use the same method here.

[25] The eddy viscosity model of *Zelt* [1991] can be written schematically,

$$u_t + uu_x + g\eta_x + R - (\nu_b u_x)_x = 0 \tag{14}$$

where u is the velocity, ν_b is the eddy viscosity, η is the free surface and R represents dispersive terms. *Zelt* [1991] further developed an expression for the eddy viscosity ν_b,

$$\nu_b = -Bl^2 u_x; \qquad l = \gamma(h+\eta), \tag{15}$$

where *Heitner and Housner* [1970] determined that the mixing length parameter $\gamma = 2$ to best fit the width of a hydraulic jump. The factor B is a breaking switch based on the spatial gradient of the velocity and its exceedence of a breaking criterion; it is formulated to provide a somewhat gradual introduction of dissipation during breaking,

$$\begin{aligned} B &= 1; u_x \le 2u_x^* \\ B &= u_x/u_x^*; 2u_x^* < u_x \le u_x^* \\ B &= 0; u_x > u_x^* \end{aligned} \tag{16}$$

with

$$u_x^* = -0.3\sqrt{g/h}. \tag{17}$$

[26] *Kennedy et al.* [2000] found that more stable estimates of ν_b are obtained by examining wave evolution in the time domain, since time stepping is often more highly resolved than spatial stepping. *Kennedy et al.* [2000] thus transformed (14) using the equation for conservation of mass. An approximation, based on the first-order relationship $u_x \approx \eta_t/h$, is adequate for our analysis of time series and is given by

$$\nu_b \approx B\gamma^2 h\eta_t \tag{18}$$

$$\begin{aligned} B &= 1; \eta_t \ge 2\eta_t^* \\ B &= \eta_t/\eta_t^* - 1; \eta_t^* \le \eta_t < 2\eta_t^* \\ B &= 0; \eta_t < \eta_t^* \end{aligned} \tag{19}$$

$$\eta_t^* = 0.3\sqrt{gh}. \tag{20}$$

[27] Finally *Kirby and Kaihatu* [1996] express the instantaneous energy dissipation as

$$\epsilon_b = -\rho hu(\nu_b u_x)_x \approx -\rho\left(\frac{\eta}{h}\right)(\nu_b\eta_t)_t. \tag{21}$$

This therefore allows us to deduce the dissipation directly from the measurements, assuming that the dissipation formulation (21) is sufficiently descriptive. *Kirby and Kaihatu* [1996] further transform (21) to a spectral form by first defining the spectral density of the free surface and the dissipation respectively as

$$S_\eta(n) = \frac{\langle |A_n|^2 \rangle}{2\Delta f} \tag{22}$$

$$S_{\epsilon_b}(n) = \frac{\langle |\hat{\epsilon}_{bn}| \rangle^2}{2\Delta f}. \tag{23}$$

We can develop an energy flux relation from (7) by first including shoaling,

$$A_{nx} + \frac{C_{gn,x}}{2C_{gn}}A_n = \alpha_n A_n, \tag{24}$$

where C_{gn} is the group velocity for the nth frequency component. Multiplying (24) by the complex conjugate amplitude A_n^*, writing an equation which is the complex conjugate of the result, adding both equations together, and then taking $C_{gn} \approx \sqrt{gh}$ (assuming shallow water), yields

$$\left(\frac{1}{2}\rho g|A_n|^2\sqrt{gh}\right)_x = -2\sqrt{gh}\alpha_n\left(\frac{1}{2}\rho g|A_n|^2\right). \tag{25}$$

Using (22) to describe the surface-displacement-based energy density in a smoothed version of (25), and (23) to describe the spectrum of fluctuations in instantaneous dissipation described by (21), leads to a relation for α_n given by

$$\alpha_n = \frac{1}{\rho g\sqrt{gh}}\frac{1}{\sqrt{2\Delta f}}\frac{\sqrt{S_{\epsilon_b}(n)}}{S_\eta(n)}. \tag{26}$$

In the time domain, the dissipation ϵ_b acts as a row of "spikes" or delta processes. This behavior translates to the frequency domain as a flat spectrum (S_{ϵ_b} has little or no frequency dependence), and thus leads to the conclusion that α_n should be proportional to $S_\eta(n)^{-1}$.

[28] We now investigate evolutionary trends in the frequency (rather than wave number) spectrum. In a previous section we noted the tendency of the high wave number range of transforming wave spectra to converge upon a k^{-2} slope, corresponding to an f^{-2} slope in shallow water. The dissipation α_n from (26) is somewhat simplistic in that we are assuming zero skewness and significant asymmetry. As noted by *Kirby and Kaihatu* [1996], there will usually be a mix of skewness and asymmetry in the wavefield.

[29] Figure 7 shows an example of the power spectrum of dissipation $S_{\epsilon_b}(f)$ for MK92 Run 1 ($h = 0.10$ m); it is clearly only weakly dependent on frequency. This tendency is seen

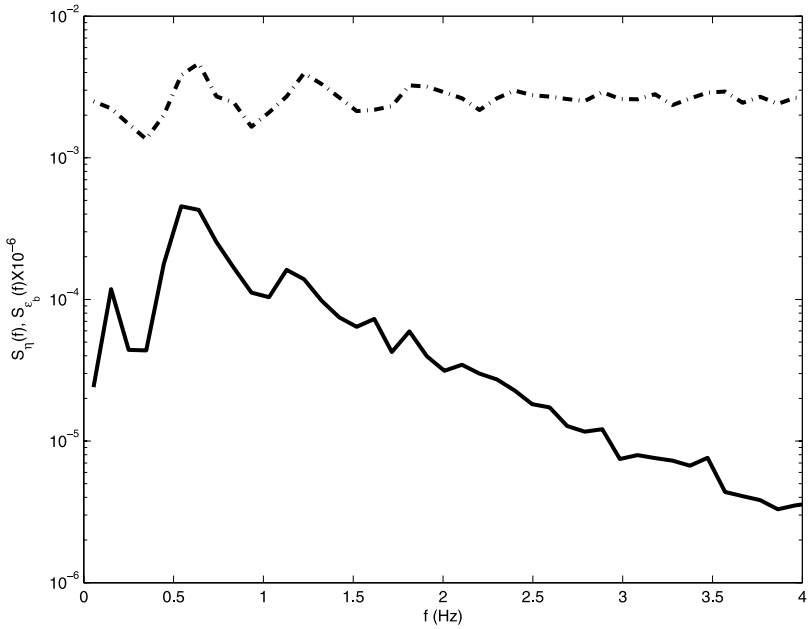

Figure 7. Power spectra of free surface elevation (solid line) and of instantaneous dissipation ϵ_b (dash-dotted line). Note that S_{ϵ_b} was divided by 10^6 to allow display on same plot.

in every data set, and was also seen by *Kirby and Kaihatu* [1996] in their analysis. Along with (26), this implies that the dissipation coefficient α_n is inversely related to the power spectrum of the free surface $S_\eta(f)$. We determined the best fit slope of both the frequency spectra and α_n for all data by using linear regression on the log of the frequency spectra and log of the frequency range $f_p \leq f \leq 0.5\, f_{Nyq}$, as well as log of the dissipation function α_n in (26). The absolute values of the slopes appear as functions of depth in Figure 8. It is clear that the inverse relationship between the slopes of the frequency spectra and the dissipation hold very well; the agreement appears to improve with decreasing water depth. Additionally, both slopes appear to converge to $f^{\pm 2}$ as the beach is approached. Nonlinear energy transfer is increasing the energy level at high frequencies during the transformation process, which decreases the slope of the tail of the spectrum. Of interest is the transformation from a rather steep tail offshore ($\sim f^{-5}$ for BK94 Case A and both MK92 runs; $\sim f^{-4}$ for BK94 Cases B and C), and toward f^{-2}. The shapes f^{-5} and f^{-3} were proposed by *Thornton* [1977] as representative shapes of the saturated tail of frequency spectra in deep and shallow water, respectively. As mentioned previously, however, it is difficult to separate natural evolution tendencies from artificial adjustments from the input wavemaker signal, so the offshore tendencies of the slopes is not validation of the spectral shapes described by *Thornton* [1977]. However, the f^{-2} shape appears to be a clear inner surf zone asymptote.

5. Discussion

[30] Thus far we have shown from analysis of the assembled data that the Zakharov range of the SV03 parameterization for wave number spectral shape compares well for most of the transformation range, but that the data uniformly show an asymptote of k^{-2} as the shoreline is approached. We have also seen a similar trend in the frequency spectra, and have related the spectral shapes to the frequency dependence of the dissipation coefficient α_n. This suggests that the k^{-2} (or f^{-2}) is a general asymptote in the inner surf zone.

[31] The approach toward this asymptote in the inner surf zone is gradual and continuous for the slope of the Toba range and quite sudden for the slope of the Zakharov range (Figure 6). We investigated the correlation between the total dissipation in the wavefield (expressed as ϵ_{brms}, the *rms* value calculated from the power spectrum $S_{\epsilon b}$ in equation (18)), the skewness (a proxy for nonlinearity) and the error in the SV03 parameterization. This error is calculated as the absolute value of percentage error between the slope calculated from data and that dictated by SV03; we denote the error in the Zakharov range as E_Z and for the Toba range as E_T. For better visualization in the comparison with skewness and ϵ_{rms}, we calculated the following:

$$\Gamma_Z = \left(1 - \overline{E_Z}\right) \tag{27}$$

$$\Gamma_T = \left(1 - \overline{E_T}\right), \tag{28}$$

where the overbar denotes normalization with the largest value in each experiment. Figure 9 shows a comparison of ϵ_{brms} and skewness (all normalized by their maximum values for the experiment) to the quantities Γ_Z and Γ_T. For all data there is a clear correlation between the location of maximum skewness and maximum dissipation ϵ_{brms}. Additionally, for all data sets except MK92 Run 2, this location also appears to match that of a maximum value of Γ_Z; the decrease in skewness and dissipation is accompanied by a decrease in Γ_Z as the spectral slope approaches k^{-2}. It appears, therefore, that the SV03 parameterization describes the spectral characteristics of wave transformation

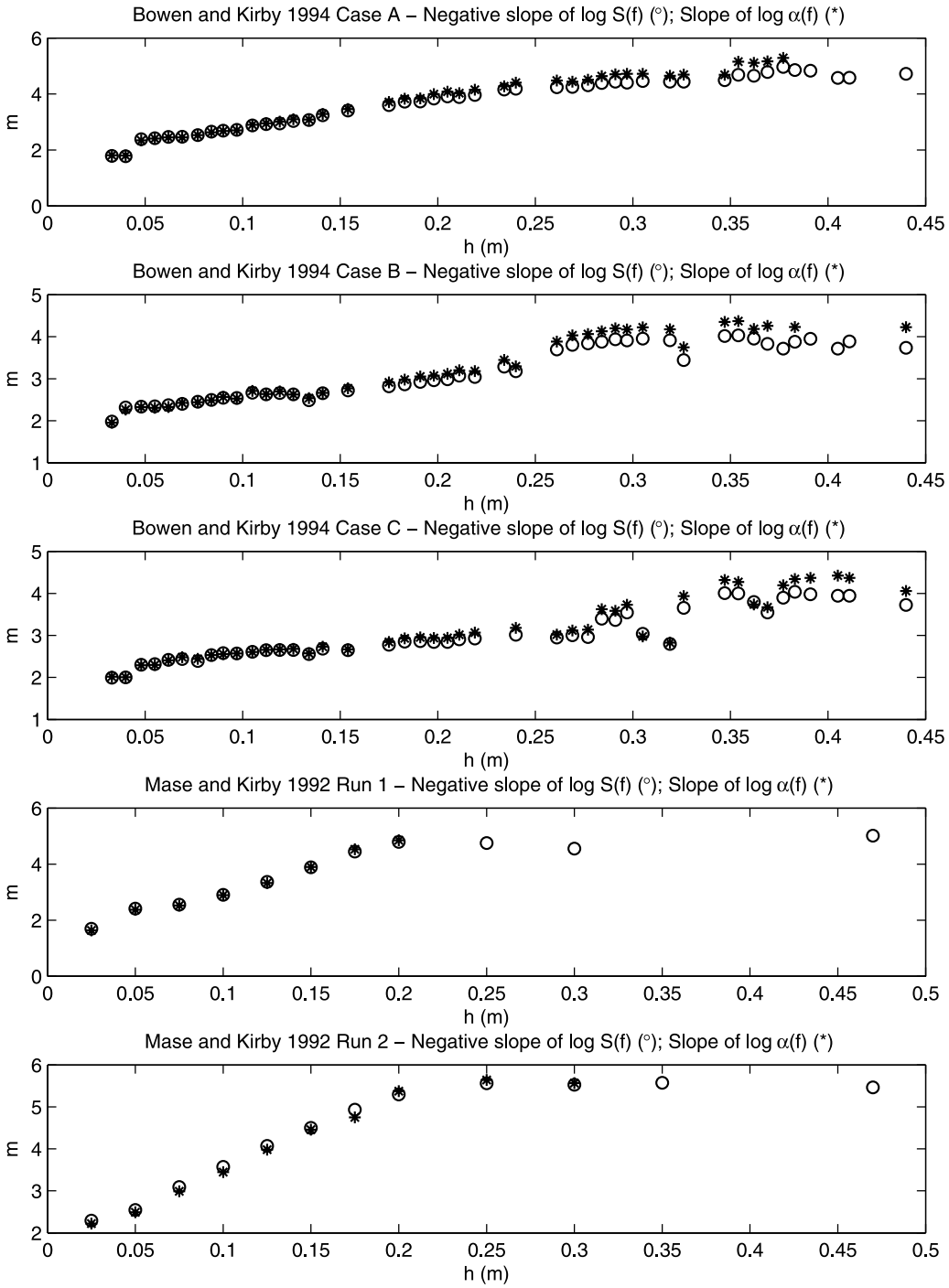

Figure 8. Comparison of slopes of the log frequency spectra of data to slope of log $\alpha(f)$ from equation (26), as a function of depth h; absolute values shown. Circles, negative slope of log $S(f)$; asterisks, slope of log $\alpha(f)$.

while the surf zone is only partially saturated. Continued breaking in the inner surf zone, however, moves the spectrum away from thermal equilibrium and toward the asymptotic shapes evident in the data. The spectral shape thus becomes more and more representative of the spectrum of sawtooth-type surf zone waves, and less in line with the equilibrium spectra parameterization of SV03.

[32] Interestingly only BK94 Cases B and C show agreement with SV03 over the majority of the experimental domain, even though data from other experiments exhibit some of the same wave parameters with worse agreement to SV03. We thus wanted to detect any correlation between the range of relative depths in the experiments and agreement with the SV03 parameterization. Figure 10 shows the discrepancy between the computed wave number slope and the parameterization as a function of μ^2, the dispersion parameter, for both Zakharov and Toba ranges. Not surprisingly, the data agrees best with the Zakharov range param-

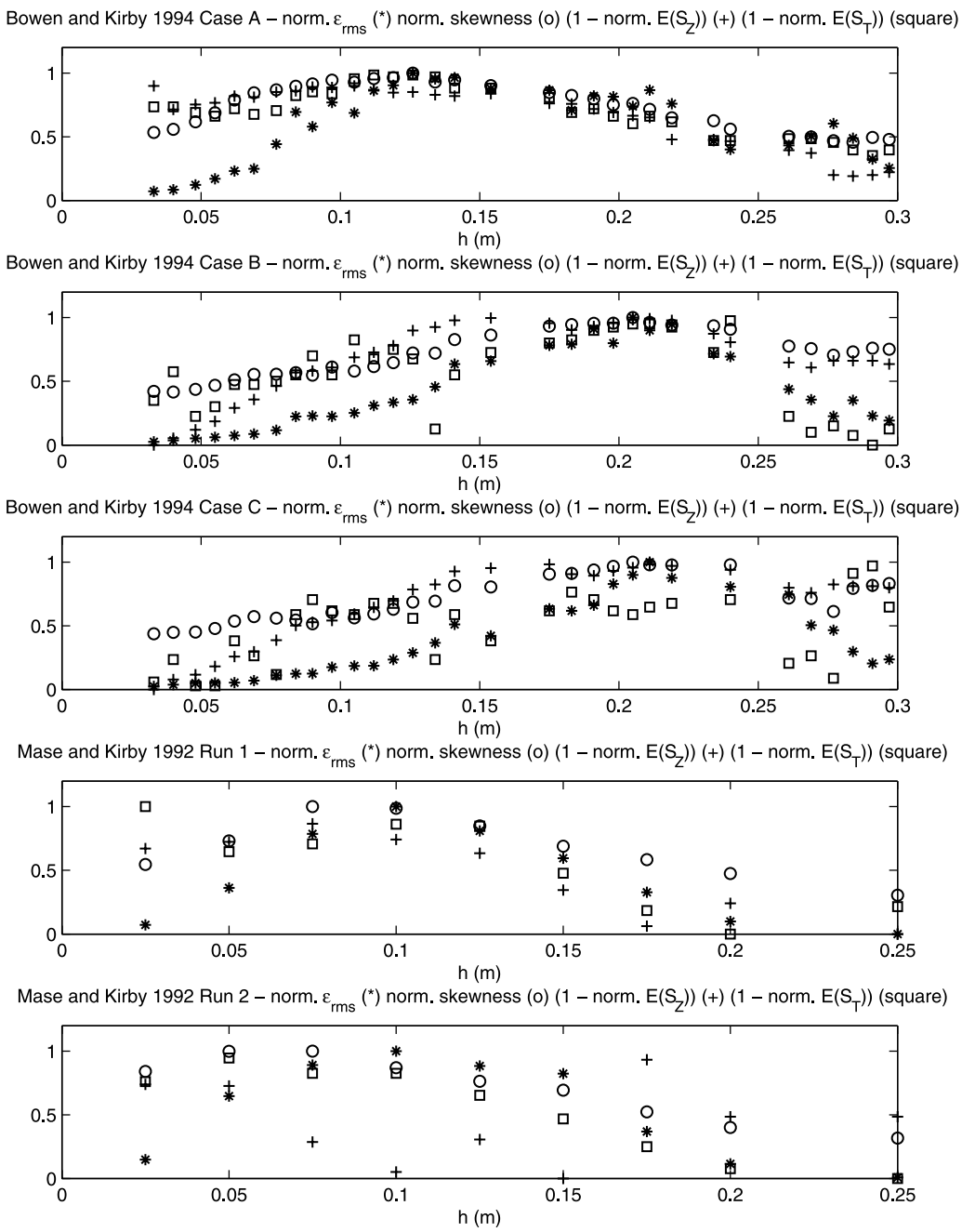

Figure 9. Comparison of root-mean-square value of ϵ_b (equation (15)) to skewness and error measure for all data sets. All values are normalized by maximum value for experiment. Asterisks, normalized ϵ_{rms}; circles, normalized skewness; pluses, Γ_Z; squares, Γ_T.

eterization for small μ^2, where the Zakharov range is most apparent. However, for very small μ^2 the error increases; this is the range in which the slope of the Zakharov range approaches k^{-2}, as seen most strikingly for BK94 Cases B and C (Figure 8). A similar trend is seen for the Toba range, which shows lower error over the entire domain than seen for the Zakharov range.

6. Summary

[33] In this paper we have investigated the evolutionary trends of frequency and wave number spectra of shoaling and breaking waves in five laboratory data sets. We have also compared these trends with prevailing theories concerning the behavior of the high-frequency and high wave number portion of the spectra. The parameterization of *Smith and Vincent* [2003] dictates that the tail of the wave number spectrum of shoaling and breaking waves have two distinct ranges and two characteristic wave number slopes. The first (Zakharov) range typically has a wave number spectral slope of $k^{-4/3}$, and which is applicable for the range $k_p \leq k < 1/h$. The second (Toba) range has a characteristic spectral slope of $k^{-5/2}$, applicable for $k > 1/h$.

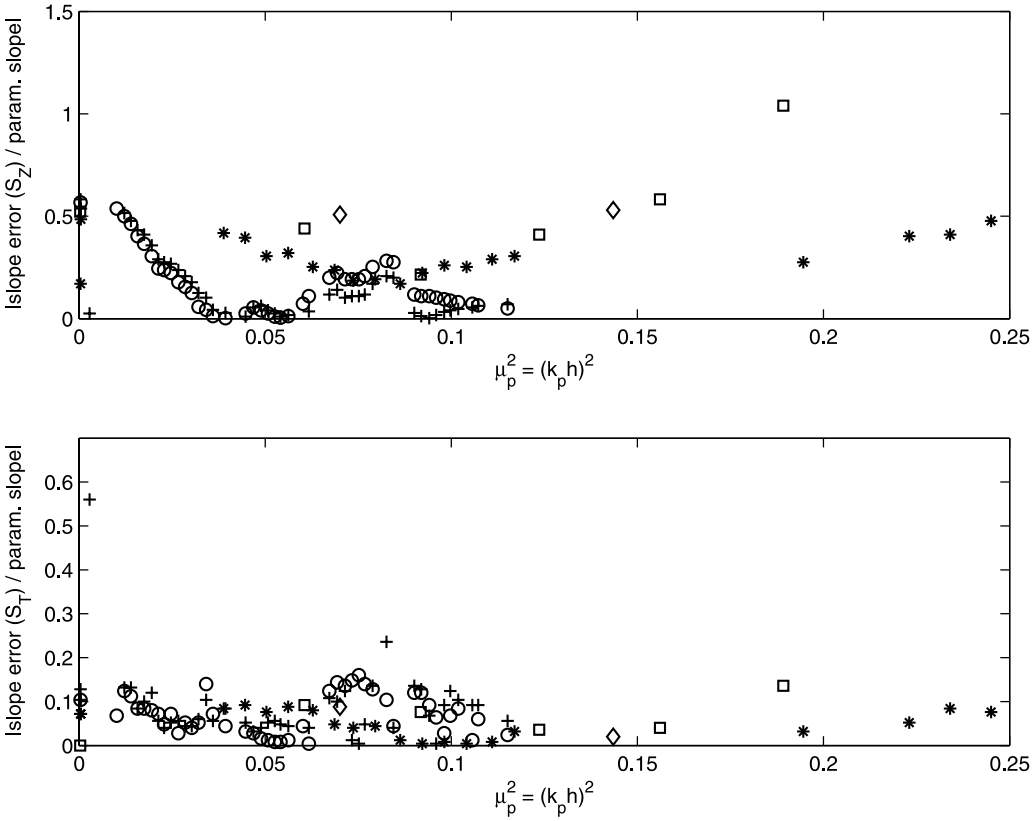

Figure 10. Comparison of error in best fit spectra slopes to SV03 parameterization as function of dispersion parameter μ_p^2. Asterisks, BK94 Case A; circles, BK94 Case B; pluses, BK94 Case C; boxes, MK92 Run 1; diamonds, MK92 Run 2. (top) Zakharov range. (bottom) Toba range.

[34] Two laboratory data sets were analyzed: *Bowen and Kirby* [1994] and *Mase and Kirby* [1992]. The combined data spans a wide range of relative water depths. Wave number spectra were calculated from frequency spectra by use of the linear dispersion relation. Comparison to the SV03 parameterization revealed that, while the overall energy level was overpredicted by the parameterization, the slopes of the log of the wave number spectra compared reasonably well to the data. Further analysis showed that the slopes calculated from the spectra of the data compared particularly well when the wavefield had reached its maximum skewness. However, as the wavefield continues into the inner surf zone, both the Zakharov and Toba range slopes depart away from their parameterized values of $k^{-4/3}$ and $k^{-5/2}$, respectively, toward k^{-2}. This is particularly evident in BK94 Cases B and C (Figure 6). This is an indication that the f^{-2} spectral shape (close to k^{-2} in shallow water) hypothesized by *Kirby and Kaihatu* [1996] is the nearshore asymptote.

[35] The instantaneous dissipation was then calculated from the data, using the method of *Kirby and Kaihatu* [1996]. The dissipation coefficient α_n in equation (26) was then determined to be related to the inverse of the shape of the frequency spectrum $S(f)$. This correspondence (Figure 8) becomes stronger in shallower water for all data sets; furthermore the asymptote f^{-2} is approached in the surf zone, confirming the contention of *Kirby and Kaihatu* [1996] that $\alpha(f) \sim f^2$. It was also mentioned that the evolutionary trends in the offshore may be artifacts of the wavemaker input; thus it is difficult to ascribe the evolution in spectral slopes in the offshore edge of the domains to any particular theory.

[36] A representative value for total dissipation ϵ_{brms} was compared to the wave skewness evolution and the error between the SV03 parameterization and the spectral slopes from data. There is a clear correlation between the location of the maximum skewness and dissipation in the wavefield, and the location of a minimum in the error in the parameterization. Both dissipation and skewness decrease as the overall energy level in the spectrum is dissipated. Correspondingly, the error of the SV03 parameterization increases, indicating that continued breaking and surf zone saturation moves the spectral shape away from equilibrium and toward the asymptotic shape k^{-2} (or f^{-2}).

[37] The notion of nonlinearity and dissipation interacting to dictate the shape of the wave spectrum may appear contrary to the finding of *Chen et al.* [1997], who determined that the shape of the power spectrum is relatively insensitive to the form of the dissipation. However, in that study, the dissipation was a priori constrained to be of a particular spectral form [*Thornton and Guza*, 1983], with the nonlinearity necessarily reacting appropriately in their Boussinesq models to maintain the iconic shape. Here we are estimating the dissipation directly from the data with no imposed frequency distribution, and intimating the behavior in concert with nonlinearity. This in essence provides strong support for the findings of *Mase and Kirby* [1992] and *Kirby and Kaihatu* [1996].

[38] From the above it is apparent that the SV03 parameterization describes the wave transformation process to a degree for a large portion of the domain. However, it appears that in the inner surf zone the f^{-2} (or k^{-2}) shape is a clear asymptote.

[39] It is interesting that the $\alpha(f) \sim f^2$ is most prevalent in the inner surf zone, and that the dependence is different in less saturated areas of the surf zone. This will affect how breaking is represented in spectral models. A future study will focus on this.

Appendix A: Spectral Forms Used in Laboratory Wave Generation

[40] The TMA spectrum [*Bouws et al.*, 1985] was used as the input spectrum for the BK94 laboratory data set. The spectral form is:

$$S(f)_{TMA} = \frac{\overline{\alpha} g^2}{(2\pi)^4 f^5} \exp\left\{ -\frac{5}{4}\left(\frac{f_p}{f}\right)^4 + (\ln\gamma)\exp\left[\frac{-(f-f_p)^2}{2\sigma^2 f_p^2}\right]\right\}\phi(f,h) \qquad \text{(A1)}$$

where $\overline{\alpha}$ is the Phillips constant (usually 0.0081), γ is the peak enhancement factor, and σ is the shape parameter:

$$\sigma = \begin{cases} \sigma_a = 0.07 & \text{if } f < f_p \\ \sigma_b = 0.09 & \text{if } f \geq f_p \end{cases}$$

and the factor $\phi(f, h)$ scales the spectrum with respect to the effect of water depth h:

$$\phi = \begin{cases} 0.5\omega_h^2 & \text{if } \omega_h < 1 \\ 1 - 0.5(2-\omega_h)^2 & \text{if } 1 \leq \omega_h \leq 2 \\ 1 & \text{if } \omega_h > 2 \end{cases}$$

where:

$$\omega_h = 2\pi f\sqrt{\frac{h}{g}}. \qquad \text{(A2)}$$

Typically, to generate a wave train of a specified significant wave height, the parameter $\overline{\alpha}$ is scaled so that the total energy in the spectrum corresponds to that wave height.

[41] The Pierson-Moskowitz spectrum, used for the MK92 laboratory experiment, was developed for a fully developed sea under a constant wind in an open ocean:

$$S(f)_{PM} = \frac{\overline{\alpha} g^2}{(2\pi)^4 f^5} \exp\left\{ -0.74\left(\frac{g}{2\pi U_{19.5} f}\right)^4 \right\} \qquad \text{(A3)}$$

where $U_{19.5}$ is the wind speed 19.5 m above the mean sea level. For the purposes of laboratory-generated waves, where there is no wind, a wind speed is chosen to provide the desired shape and again the parameter $\overline{\alpha}$ scaled to yield the desired significant wave height.

[42] **Acknowledgments.** J. M. K., J. V., and K. L. E. were supported by the Office of Naval Research through the Naval Research Laboratory Base Program 6.1 project "Nonlinear Interactions in Nearshore Environments (NINE)." J. T. K. was supported by the Office of Naval Research Physical Oceanography program through the project "Directional, Dissipative and Random Effects in Breaking Waves." The authors thank Glenn Bowen for full access and unrestricted use of the Bowen and Kirby data. J. M. K. thanks Jane McKee Smith and Zeki Demirbilek of the Coastal and Hydraulics Laboratory, U.S. Army Engineering Research and Development Center, Vicksburg, Mississippi, for providing office space in the wake of Hurricane Katrina, without which this paper would not have been completed in a timely manner. This is NRL publication NRL/JA/7320-05-5335 and has been approved for public release; distribution unlimited.

References

Agnon, Y., and A. Sheremet (1997), Stochastic nonlinear shoaling of directional spectra, *J. Fluid Mech.*, *345*, 79–99.

Agnon, Y., A. Sheremet, J. Gonsalves, and M. Stiassnie (1993), Nonlinear evolution of a unidirectional shoaling wave field, *Coastal Eng.*, *20*, 29–58.

Battjes, J. A., and J. P. F. M. Janssen (1978), Energy loss and set-up due to breaking of random waves, paper presented at 16th International Conference on Coastal Engineering, Am. Soc. of Civ. Eng., Hamburg, Germany.

Bouws, E., H. Gunther, W. Rosenthal, and C. L. Vincent (1985), Similarity of the wind spectrum in finite depth water: 1. Spectral form, *J. Geophys. Res.*, *90*(C1), 975–986.

Bowen, G. D., and J. T. Kirby (1994), Shoaling and breaking random waves on a 1:35 laboratory beach, *Tech. Rep. CACR-94-14*, Cent. for Appl. Coastal Res., Dep. of Civ. Eng., Univ. of Del., Newark.

Chen, Y., and P. L.-F. Liu (1995), Modified Boussinesq equations and associated parabolic models for water wave propagation, *J. Fluid Mech.*, *288*, 351–381.

Chen, Y., R. T. Guza, and S. Elgar (1997), Modeling spectra of breaking surface waves in shallow water, *J. Geophys. Res.*, *102*(C11), 25,035–25,046.

Eldeberky, Y., and J. A. Battjes (1995), Parameterization of triad interaction in wave energy models, paper presented at Coastal Dynamics '95, Am. Soc. of Civ. Eng., Gdansk, Poland.

Eldeberky, Y., and J. A. Battjes (1996), Spectral modeling of wave breaking: Application to Boussinesq equations, *J. Geophys. Res.*, *101*(C1), 1253–1264.

Eldeberky, Y., and P. A. Madsen (1999), Deterministic and stochastic evolution equations for fully-dispersive and weakly nonlinear waves, *Coastal Eng.*, *28*, 1–24.

Elgar, S., M. H. Freilich, and R. T. Guza (1990a), Recurrence in truncated Boussinesq models for nonlinear waves in shallow water, *J. Geophys. Res.*, *95*(C7), 11,547–11,556.

Elgar, S., M. H. Freilich, and R. T. Guza (1990b), Model-data comparisons of moments of nonbreaking shoaling surface gravity waves, *J. Geophys. Res.*, *95*(C9), 16,055–16,063.

Freilich, M. H., and R. T. Guza (1984), Nonlinear effects on shoaling surface gravity waves, *Philos. Trans. R. Soc., Ser. A*, *311*, 1–41.

Heitner, K. L., and G. W. Housner (1970), Numerical model for tsunami runup, *J. Waterw. Port Coastal Ocean Eng.*, *96*, 701–719.

Herbers, T. H. C., and M. C. Burton (1997), Nonlinear shoaling of directionally spread waves on a beach, *J. Geophys. Res.*, *102*(C9), 21,101–21,114.

Hoefel, F., and S. Elgar (2003), Wave-induced sediment transport and sandbar migration, *Science*, *299*, 1885–1887.

Kaihatu, J. M. (2001), Improvement of parabolic nonlinear dispersive wave model, *J. Waterw. Port Coastal Ocean Eng.*, *127*, 113–121.

Kaihatu, J. M., and J. T. Kirby (1995), Nonlinear transformation of waves in finite water depth, *Phys. Fluids*, *7*(8), 1903–1914.

Kaihatu, J. M., and J. T. Kirby (1998), Two-dimensional parabolic modeling of extended Boussinesq equations, *J. Waterw. Port Coastal Ocean Eng.*, *124*, 57–67.

Kennedy, A. B., Q. Chen, J. T. Kirby, and R. A. Dalrymple (2000), Boussinesq modeling of wave transformation, breaking, and run-up. I: 1D, *J. Waterw. Port Coastal and Ocean Eng.*, *126*, 39–47.

Kirby, J. T., and J. M. Kaihatu (1996), Structure of frequency domain models for random wave breaking, paper presented at 25th International Conference on Coastal Engineering, Am. Soc. of Civ. Eng., Reston, Va.

Kitaigorodskii, S. A. (1983), On the theory of the equilibrium range in the spectrum of wind-generated gravity waves, *J. Phys. Oceanogr.*, *13*, 816–827.

Kofoed-Hansen, H., and J. H. Rasmussen (1998), Modelling of nonlinear shoaling based on stochastic evolution equation, *Coastal Eng.*, *33*, 203–232.

Lescinski, J. L., H. T. Özkan-Haller, and S. M. Henderson (2003), Predictions of onshore sandbar movement using near-bed velocities: Comparison with

DUCK94 data, *Eos Trans. AGU*, *84*(52), Ocean Sciences Meet. Suppl., Abstract OS31G-09.
Madsen, P. A., R. Murray, and O. R. Sørensen (1991), A new form of Boussinesq equations with improved dispersion characteristics, *Coastal Eng.*, *15*, 371–388.
Mase, H., and J. T. Kirby (1992), Hybrid frequency-domain KdV equation for random wave transformation, paper presented at 23rd International Conference on Coastal Engineering, Am. Soc. of Civ. Eng., Venice, Italy.
Nwogu, O. (1993), An alternative form of the Boussinesq equations for nearshore wave propagation, *J. Waterw. Port Coastal Ocean Eng.*, *119*, 618–638.
Phillips, O. M. (1958), The equilibrium range in the spectrum of wind-generated waves, *J. Fluid Mech.*, *4*, 426–434.
Resio, D. T., J. H. Pihl, B. A. Tracy, and C. L. Vincent (2001), Nonlinear energy fluxes and the finite depth equilibrium range in wave spectra, *J. Geophys. Res.*, *106*(C4), 6985–7000.
Smith, J. M., and C. L. Vincent (1992), Shoaling and decay of two wave trains on beach, *J. Waterw. Port Coastal Ocean Eng.*, *118*, 517–533.
Smith, J. M., and C. L. Vincent (2003), Equilibrium ranges in surf zone wave spectra, *J. Geophys. Res.*, *108*(C11), 3366, doi:10.1029/2003JC001930.
Thornton, E. B. (1977), Rederivation of the saturation range in the frequency spectrum of wind-generated gravity waves, *J. Phys. Oceanogr.*, *7*, 137–140.
Thornton, E. B., and R. T. Guza (1983), Transformation of wave height distribution, *J. Geophys. Res.*, *88*(C10), 5925–5938.
Toba, Y. (1973), Local balance in the air-sea boundary processes on the spectrum of wind waves, *J. Oceanogr. Soc. Jpn.*, *29*, 209–220.
Wei, G., J. T. Kirby, S. T. Grilli, and R. Subramanya (1995), A fully nonlinear Boussinesq model for surface waves. I. Highly nonlinear, unsteady waves, *J. Fluid Mech.*, *294*, 71–92.
Zakharov, V. (1999), Statistical theory of gravity and capillary waves on the surface of a finite-depth fluid, *Eur. J. Mech. B FLuids*, *18*, 327–344.
Zelt, J. A. (1991), The run-up of nonbreaking and breaking solitary waves, *Coastal Eng.*, *15*, 205–246.

K. L. Edwards, Oceanography Division, Code 7322, Naval Research Laboratory, Stennis Space Center, MS 39529-5004, USA.
J. M. Kaihatu, Zachry Department of Civil Engineering, Texas A&M University, College Station, TX 77843-3136, USA. (jkaihatu@civil.tamu.edu)
J. T. Kirby, Center for Applied Coastal Research, University of Delaware, Newark, DE 19716, USA.
J. Veeramony, Advanced Systems Group, Jacobs Technology Inc., Stennis Space Center, MS 39529, USA.